Optics Letters

Closed-loop technique based on gain balancing for real-time Brillouin optical time-domain analysis

Li Zhang,[1,*] Ana Gabriela Correa-Mena,[1] Zhisheng Yang,[1,2] Florian Sauser,[3] Sébastien Le Floch,[3] and Luc Thévenaz[1]

[1]Ecole Polytechnique Fédérale de Lausanne, Group for Fibre Optics, SCI-STI-LT Station 11, 1015 Lausanne, Switzerland
[2]Present address: State Key Laboratory of Information Photonics & Optical Communications, Beijing University of Posts and Telecommunications, Beijing 100876, China
[3]Haute Ecole ARC Ingénierie (University of Applied Sciences of Western Switzerland), Rue de la Serre 7, 2610 Saint-Imier, Switzerland
*Corresponding author: li.zhang@epfl.ch

A closed-loop servo control based on balancing the gain of two probing frequencies is proposed for real-time Brillouin optical time-domain analysis (BOTDA) without post-processing. With the most basic BOTDA hardware setup, the system can perform measurement in 150 ms and track a sudden Brillouin frequency shift (BFS) change in excess of 300 MHz (corresponding to a temperature change of more than 250°C) over ~5 km of fiber with a spatial resolution of 2 m. Moreover, the feedback loop is independent of the loss experienced by the probe and pump, with no requirement on the BFS uniformity along the fiber. All these advantages make the proposed system suitable for field applications in harsh environments.

Introduction. Distributed fiber sensing has drawn constant attention since its advent owing to the unique advantages of optical fiber, such as low loss, electromagnetic immunity, and absence of chemical reactivity [1]. This technique is therefore the perfect sensing candidate for large-structure health monitoring [2–4] in harsh environments, thus requiring high robustness and agility of the sensing system. Namely, the system should be robust against fiber loss or pump/probe power change and a large measurement dynamic range is preferred.

As one of the most investigated distributed fiber sensors, Brillouin optical time-domain analysis (BOTDA) is often used to measure the local temperature/strain experienced by a sensing fiber through the change of the Brillouin frequency shift (BFS) by probing the local Brillouin gain spectra (BGS). One drawback of BOTDA is the measurement (tens of seconds) [5] due to the step-by-step frequency scanning process that must be completed before extracting the BGS. Several schemes have been proposed to circumvent this frequency scanning including using optical frequency comb [6] or chirp chain [7] as the probe and demodulation through the Brillouin phase shift rather than the BFS [8], to cite some of them.

Alternatively, the most widespread method interrogates through a probe frequency positioned on the slope of the BGS and measures the Brillouin gain amplitude change because this approach does not add any significant complexity to the system setup [9–11]. However, to enlarge the dynamic range, the measurement speed is scaled down by the number of probe tones. In a fully distinct approach, a closed-loop BOTDA has been proposed [12], where at each location along the fiber an independent feedback loop is implemented, so that the probe frequency is actually *tracking* the BFS change and the feedback loop is dynamically self-adapting to any variations of BFS distribution over the sensing fiber. However, this fast and precise BOTDA still shows a response not totally immune to pump/probe power changes.

A real-time BOTDA system is here proposed, based on a fully classical and basic optical configuration and showing a large dynamic range and a high robustness. It interrogates a fiber with two successive chains of a frequency-coded probe, where the probe frequencies can be individually set for each location, similar to that reported in Ref. [12]. To keep the balance of the Brillouin gain of the two frequencies, a corrective factor can be calculated for the probe frequencies that are updated using this feedback loop, with a large immunity to any pump/probe power change. This is made possible by using a fast frequency-agile microwave generator that can switch to a new frequency at a nanosecond rate to build the proper dynamic probe chain. Temperature sensing and dynamic strain sensing have been achieved using the most classical BOTDA optical layout.

Principle. The local Brillouin gain measured through conventional BOTDA at position z in the fiber is

$$g_B(\nu, z) = g(\nu, z)P_{\text{pump}}\Delta z/A_{\text{eff}}, \qquad (1)$$

where P_{pump}, Δz, and A_{eff} are the peak power of the pump pulse, the interaction length, and the nonlinear effective area of the guided mode of the interaction length [13]. The local BGS $g(\nu, z)$ is

$$g(\nu, z) = g_0(z)\frac{(\Delta\nu_B/2)^2}{(\nu - \Delta\nu_B)^2 - (\Delta\nu_B/2)^2}, \qquad (2)$$
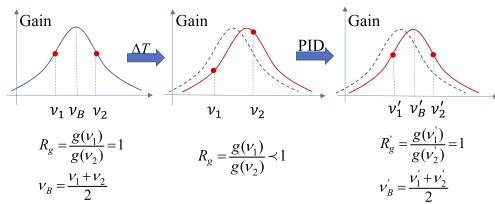
Fig. 1. Tracking principle of operation of the PID based on the gain ratio at two frequencies.

where ν, $g_0(z)$, and Δ_B are the detuning frequency of the probe with respect to the Brillouin frequency shift ν_B, the Brillouin gain coefficient, and the half width at half maximum.

A closed-loop BOTDA has been proposed in Ref. [12], where its probe is not frequency-scanned but locked on the slope of the BGS (*tracking*). As a result, the measurement time is reduced significantly; however, since the feedback loop relies on the absolute value of the response $g_B(\nu, z)$, it is impossible for the proportional–integral–derivative controller (PID) to know whether the change of the measured gain is caused by the change of ν_B or the change of pump power. Moreover, an initial full scan of the BGS is required to obtain a preset BFS distribution.

In the present work, the principle of the feedback loop is based on a double-frequency probing and is sketched in Fig. 1. For an arbitrary position z in the fiber, the Brillouin sensing system is consecutively probing the BGS at two different frequencies $\nu_1(t, z)$ and $\nu_2(t, z)$ positioned on the slope of the local BGS. We define $\nu_2(t, z) - \nu_1(t, z) = 2\Delta\nu$, where $\Delta\nu$ is the constant frequency offset from the assumed peak gain. As a result, the second probe frequency chain is simply a replicate of the first probe chain, shifted in frequency by $2\Delta\nu$. Assuming that the obtained Brillouin gains are $g_B(\nu_1(t, z))$ and $g_B(\nu_2(t, z))$, respectively, the ratio between both gains is simply $R_g(t, z) = \frac{g(\nu_1(t, z))}{g(\nu_2(t, z))}$, where the P_{pump} term is canceled out in the fraction.

In this system, we lock the operating point at $R_g(t, z) = 1$, which means that the two probing frequencies are equidistant, but on opposite sides of $\nu_B(t, z)$ according to Eq. (2) (*balancing*). So $\nu_B(t, z) = \frac{\nu_1(t, z) + \nu_2(t, z)}{2}$. When the local Brillouin spectrum shifts owing to a temperature/strain change, the two probes are thus no longer symmetrically positioned with respect to the new BFS, and the ratio $R_g(t, z)$ changes. After being processed by a software-implemented PID to calculate the correction to be applied on the frequency, the local dual probe frequencies are jointly shifted to new spectral positions where the new gain ratio $R'_g(t, z)$ tends toward 1. The system dynamically reaches this target value after a limited number of cycles.

Experimental setup. A basic-structure BOTDA as shown in Fig. 2 is built to verify the proposed technique. A coupler splits the light from a distributed feedback (DFB) laser into pump and probe branches. Light in the upper branch (probe) is intensity modulated in carrier-suppressed mode by an electro-optic modulator (EOM) to deliver a two-tone signal spectrum; then the obtained signal with two spectral lines is launched into the fiber under test (FUT) through an optical isolator. In the other branch, the laser light is shaped into a 20 ns square pump pulse by a semiconductor optical amplifier (SOA). A polarization scrambler is inserted to mitigate the polarization dependence of the Brillouin gain. The pump pulse is then amplified by an erbium-doped fiber amplifier (EDFA) and launched into the fiber through an optical circulator. On the detection side, a fiber Bragg grating (FBG) and an optical circulator are used to allow only the lower-frequency
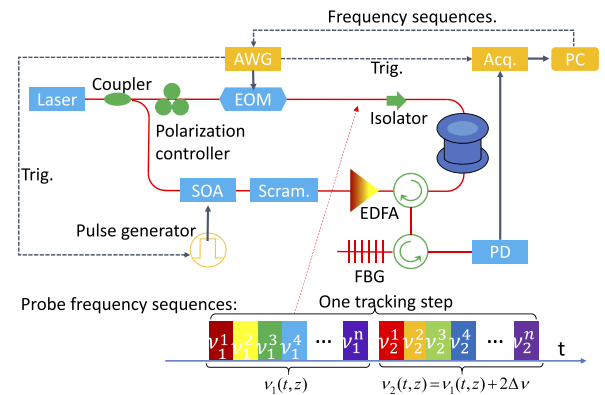
Fig. 2. Experimental setup. (EOM: electro-optic modulator; SOA: semiconductor optical amplifier; Scram.: polarization scrambler; EDFA: erbium-doped fiber amplifier; FBG: fiber Bragg grating; PD: photodetector (125 MHz bandwidth); Acq.: acquisition card (150 MS/s); PC: personal computer; AWG: arbitrary wave generator; Trig.: trigger.)

probe tone to reach the photodetector (PD). The electric signal is then digitized by an acquisition card. A digital re-sampling is implemented to form a point-to-point pair for the acquired trace and the probe segments. The calculations of $R_g(z)$ and the corresponding frequency shift are made after the acquisition of both averaged traces using dedicated controlling software. The updated frequency trains ($\nu_1(t, z)$ and $\nu_2(t, z)$) are then uploaded to a custom-made arbitrary wave generator (AWG) that drives the EOM before each sensing operation.

A key feature of this technique is that, instead of probing the entire fiber using a sequence of constant optical frequencies, the probe light consists of many segments with their own frequency, as shown in Fig. 2: the length of each segment matches the pump pulse (20 ns in the experiment), so that the pump interacts with only one probe segment at a given spatially resolved position. An independent feedback loop must therefore be implemented for each interacting segment (or spatially resolved position). Even in the case of a non-uniform BFS distribution along the fiber, as in real situations in the field, each position is locked independently, so that the local temperature and strain change can be properly tracked. An averaging of 256 is implemented to improve the signal-to-noise ratio. We define the whole iteration of probing with $\nu_1(t, z)$ and $\nu_2(t, z)$ and the associated correction calculations as one *tracking step*. When the FUT is around 1 km long, around 1000 (2×(fiber length 1000 m)/(spatial resolution 2 m)) segments are uploaded to the AWG during each tracking step. Each step lasts 150 ms in our implementation, mainly limited by the uploading time from the computer to the customized AWG that is connected via a serial connection with a baud rate of 921,600, and the uploading time is linearly proportional to the fiber length. The uploading speed can be further improved by upgrading the connection.

Results. As demonstrated in Ref. [12], the detuning from the peak gain frequency $\Delta\nu$ must be 17.3 MHz to maximize the slope of the gain $\eta(\Delta\nu) = \frac{\mathrm{d}Gain(\nu_1)}{\mathrm{d}\Delta\nu}$. We set the PID proportional parameter $P = 1/(16\eta)$ and its integral parameter $I = P/200$ with an initial guess that ν_B equals 10.75 GHz, which is not too far from the general BFS value of a standard single-mode fiber (~10.8 GHz at room temperature). This means the initial $\nu_1(z)$ and $\nu_2(z)$ are 10.75±0.0173 GHz, respectively. The evolution of $\nu_1(z)$, $\nu_2(z)$, $g(\nu)$, and R_g as a function of position is shown in
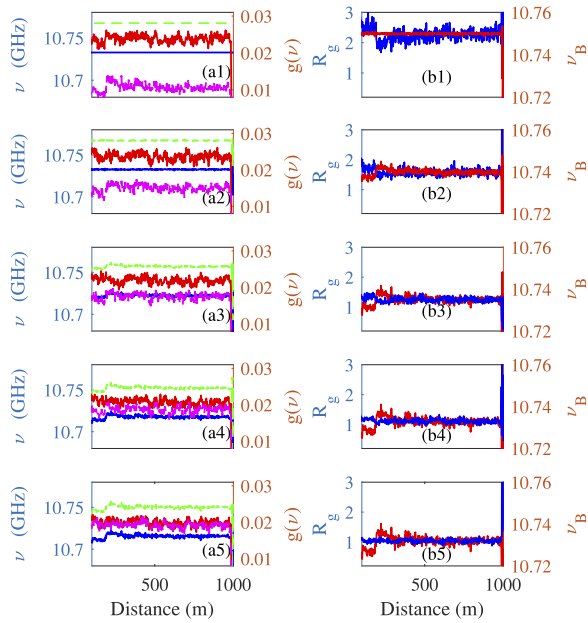
Fig. 3. Observations of the gain evolution on the first, third, fifth, seventh, and ninth tracking steps. (a) Set ν_1 (blue), ν_2 (dashed green), obtained Brillouin gain $g(\nu_1)$ (red), and $g(\nu_2)$ (pink). (b) Obtained Brillouin gain ratio R_g (blue) and calculated ν_B (red).

Fig. 3. It can be seen that, for the first tracking step, the initial frequencies are constant but not the Brillouin gain along the fiber, since the BFS of the fiber is not uniform, probably as a result of the different coiling tension. $Gain(\nu_1(z))$ and $Gain(\nu_2(z))$ are significantly different in Fig. 3(a1) since the two probes are not in gain-equalizing spectral positions with respect to the real BFS of the fiber. In Fig. 3(b1) the calculated gain ratio R_g is also not uniform which results in a new guess of ν_B sequences depicted by the red line. The modulation frequency sequences $\nu_1(z)$ and $\nu_2(z)$ in the AWG are then updated accordingly. As the probe frequencies are sequentially updated, the two gain traces tend to be equal and gradually uniform over the entire fiber length; see Figs. 3(a5) and 3(b5).

The measured BFSs of the whole fiber through the proposed scheme are shown in Fig. 4(a), in comparison with the BFS obtained via the conventional BOTDA using the same hardware structure (scan step: 1 MHz; scan range: 300 MHz). The two traces show a perfect match. It should be noted from the inset in Fig. 4(a) that, despite the oscillation around the beginning (150–250 m), the BFS profile is well reconstructed without any pre-calibration. To further demonstrate the self-calibration property of the system, we repeat the same experiment while replacing the FUT by three appended fibers (Fibers A, B, and C), and their Brillouin shifts at room temperature are 10.86 GHz, 10.55 GHz, and 10.73 GHz, respectively. The results are shown in Fig. 4(b). The BFS of Fiber A is ~300 MHz away from that of Fiber B and would require a large scanning range using a conventional BOTDA to acquire the whole BGS distribution. Here the proposed tracking scheme is still able to track and measure this distant BFS with the same initial sequence centered at 10.75 GHz without any frequency scan, proving a remarkable locking range. It can be seen that in Fig. 4(b), the Brillouin shifts of Fiber A and Fiber C are quickly measured, and eventually after 200 steps of correction, ν_B of Fiber B is measured, which is 200 MHz away from the initial guess. The large dynamic range can
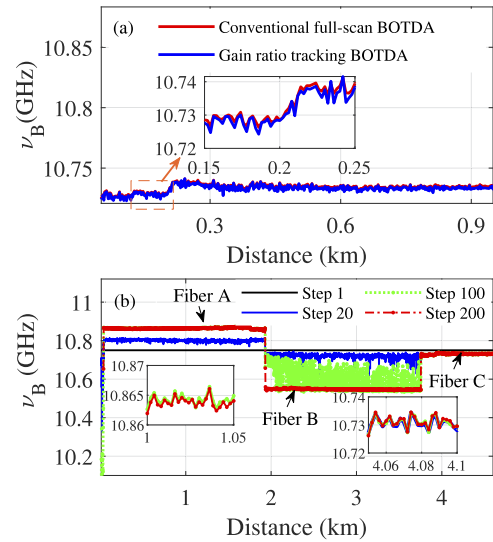
Fig. 4. (a) Comparison between conventional BOTDA and gain ratio tracking BOTDA. (b) BFSs of three appended fibers obtained by the gain ratio tracking BOTDA ($P = 1/(16\eta)$, $I = P/200$).
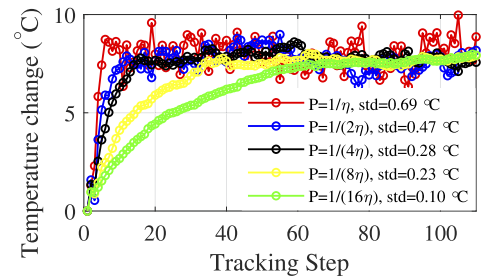
Fig. 5. Response of the system with different proportional gains (P).

be explained by the fact that the gain ratio R_g is a monotonic function of ν over the whole spectral range.

Thorough investigations of the impact of PID setting can be found in Ref. [12,14]. Actually, according to the sensing requirement in terms of the measurement speed and accuracy, the system can be customized by tuning the PID parameters. Here, we demonstrate the system's flexibility in measurement accuracy and speed by tuning the proportional gain P. We use Fiber C as the FUT, and 10 m of the FUT from 995 m to 1005 m is taken out from the fiber spool and placed into a thermal bath to play the role of a hot spot. A step temperature change of 8 K is applied at the hot spot, and the successive corrected temperature is shown for each tracking step in Fig. 5. We can see that a smaller P results in a slower response but a higher accuracy. For example, only 3 steps are needed to determine the new temperature when $P = 1/\eta$ and the corresponding accuracy is 0.69 K (each step takes ~150 ms); while around 60 steps are required when $P = 1/(16\eta)$, resulting in an accuracy of 0.10 K.

Two experiments have been conducted to check the sensing performance. The water temperature is changed by 6 K. We set a relatively small $P = 1/(16\eta)$ (and add an integral part $I = P/200$ according to Ref. [12]) in order to get a higher accuracy. The temperature distribution along the fiber is shown in Fig. 6(a), which clearly and accurately resolves the 6 K temperature change at the hot spot and the accuracy is 0.14 K. Secondly, we set $P =$
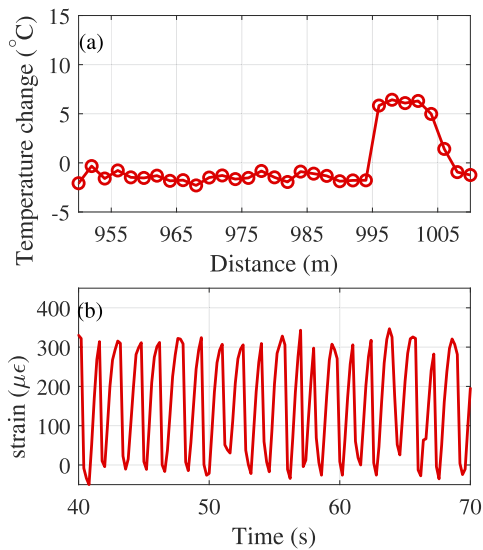
Fig. 6. (a) Temperature sensing ($P = 1/(16\eta)$, $I = P/200$), using BFS obtained by conventional BOTDA as a reference. (b) Dynamic strain sensing ($P = 1/\eta$).
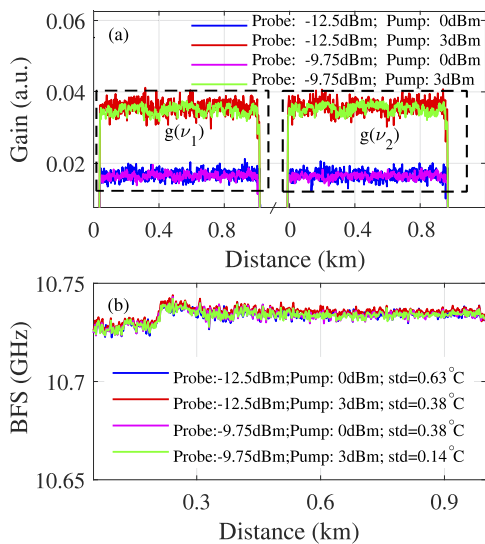
Fig. 7. Output of the tracking system with different probe/pump powers. (a) Observed Brillouin gain. (b) Observed BFS ($P = 1/(16\eta)$, $I = P/200$).

$1/\eta$ to favor the measurement speed. A dynamic strain change is applied to 2 m of the fiber at a distance of 993 m by stretching this fiber segment using a connecting rod driven by an electric motor. The obtained strain change is illustrated in Fig. 6(b) where the acquisition rate is ∼2.2 Hz.

To verify the resistance of the system to a probe/pump power change, we operate the sensing system in four different power settings and the results are illustrated in Fig. 7. Although the observed gain is dependent on the pump power [as shown in Fig. 7(a)], the BFS over the entire 1 km fiber can be retrieved successfully in four different power regimes with a decreased accuracy when the probe/pump power is decreased.

It should be noted that the measurement time is not increased compared with the system in Ref. [12] to maintain the same BFS accuracy. This is because two Brillouin gain traces are

obtained and used for the BFS estimation at each step. Thus only half of the averaging number is required to keep the same signal-to-noise ratio of the gain trace.

Conclusions. A closed-loop BOTDA based on Brillouin gain balancing is proposed for the first time. The feedback loop response and parameters are independent of the pump and probe powers and the system delivers a fully accurate quantitative value of the BFS in conditions close to real time, with the full BFS distribution updated at each step and without strict conditions on the initial uniformity of the fiber. Unlike the slope-assisted BOTDA, the system here interrogates the local Brillouin gain with two consecutive probe frequency sequences, so that each location has an independent feedback loop, enlarging the BFS dynamic range significantly. There is a trade-off between response speed and BFS accuracy like in traditional systems, though with less time penalty than the square dependence of time averaging. Thus, without adding any complexity to the hardware of a basic BOTDA and at the expense of a specific AWG, the technique is proved fast and robust over the entire sensing fiber, with an accuracy fully equivalent to that of a traditional frequency-scanning configuration and large dynamic range.

Disclosures. The authors declare no conflicts of interest.

Data availability. Data underlying the results presented in this paper are not publicly available at this time but may be obtained from the authors upon reasonable request.

REFERENCES

1. P. Lu, N. Lalam, M. Badar, B. Liu, B. T. Chorpening, M. P. Buric, and P. R. Ohodnicki, Appl. Phys. Rev. **6**, 041302 (2019).
2. A. Minardo, E. Catalano, A. Coscetta, G. Zeni, L. Zhang, C. Di Maio, R. Vassallo, R. Coviello, G. Macchia, L. Picarelli, and L. Zeni, Remote Sens. **10**, 1291 (2018).
3. M. Aufleger, M. Conrad, T. Strobl, A. H. Malkawi, and Y. Duan, in Roller Compacted Concrete Dams, (CRC Press, 2018), pp. 401.
4. D. Zhang, J. Wang, P. Zhang, and B. Shi, Measurement **97**, 234 (2017).
5. Y. Peled, A. Motil, and M. Tur, Opt. Express **20**, 8584 (2012).
6. C. Jin, N. Guo, Y. Feng, L. Wang, H. Liang, J. Li, Z. Li, C. Yu, and C. Lu, Opt. Express **23**, 5277 (2015).
7. D. Zhou, Y. Dong, B. Wang, C. Pang, D. Ba, H. Zhang, Z. Lu, H. Li, and X. Bao, Light: Sci. Appl. **7**, 32 (2018).
8. J. Urricelqui, A. Zornoza, M. Sagues, and A. Loayssa, Opt. Express **20**, 26942 (2012).
9. Y. Peled, A. Motil, L. Yaron, and M. Tur, Opt. Express **19**, 19845 (2011).
10. A. Motil, O. Danon, Y. Peled, and M. Tur, IEEE Photonics Technol. Lett. **26**, 797 (2014).
11. D. Ba, B. Wang, D. Zhou, M. Yin, Y. Dong, H. Li, Z. Lu, and Z. Fan, Opt. Express **24**, 9781 (2016).
12. Z. Yang, M. A. Soto, D. M. Chow, P. Ray, and L. Thévenaz, J. Lightwave Technol. **36**, 1239 (2018).
13. M. A. Soto and L. Thévenaz, Opt. Express **21**, 31347 (2013).
14. K. J. Åström and T. Hägglund, J. Process Control **14**, 635 (2004).